ELSEVIER

Chemical Engineering Journal 76 (2000) 115–125

Chemical Engineering Journal

www.elsevier.com/locate/cej

A package for thermal parametric pumping adsorptive processes

R.R. Davesac [a], L.T. Pinto [a], F.A. da Silva [b], L.M. Ferreira[b,1], A.E. Rodrigues [b,*]

[a] *Department of Chemical Engineering, Universidade Federal de Santa Catarina, Florianópolis, SC, Brazil*

[b] *Laboratory of Separation and Reaction Engineering, Faculty of Engineering, University of Porto, 4050-123 Porto, Portugal*

Received 19 January 1999; received in revised form 1 August 1999; accepted 9 August 1999

Abstract

Thermal parametric pumping is a cyclic adsorptive process based on cyclic changes in the bed temperature simultaneously with flow reversal. Simplified models are adequate to describe these cyclic processes with long cycle times. Two simplified models are used here: Model I is an equilibrium model plus axial dispersion and Model II accounts for intraparticle mass transfer with LDF approximation. Simulations used parameter values obtained for the system phenol/water/ adsorbent resin Duolite ES861. Model validation is carried out by performing experiments in a pilot plant with the system phenylalanine/water/polymeric adsorbent SP206 and using published experimental data for the system phenol/water/adsorbent resin Duolite ES861. A user-friendly package 'Visual Pumping' (VP) is developed in Visual Basic for the simulation of thermal parametric pumping processes with educational and training purposes.

1. Introduction

The parametric pumping process was first described by Wilhelm et al. [30,31] as a dynamic separation process based on the differences in the adsorption equilibrium caused by a cyclic change of a thermodynamic variable (temperature, pressure, pH) simultaneously with flow reversal. In thermal parametric pumping, the temperature change can be imposed through the bed jacket in direct mode or through temperature change of the fluid stream in recuperative mode [29].

The process to be addressed here is thermal parametric pumping in the recuperative mode operating in a semi-continuous way, with feed at the top of the column. Each operation includes a series of cycles, starting with the hot cycle in upward flow and then the cold cycle in downward flow. A typical cycle starts with the bed equilibrated with the feed solution at the cold temperature and the top reservoir containing the feed solution.

Fig. 1 shows the experimental setup existing at the LSRE (Laboratory of Separation and Reaction Engineering) and described in detail elsewhere [9].

Fig. 2 illustrates the semi-continuous mode of the parametric pumping operation, when the objective is to concentrate the top product. Since the feed solution should not be added to the same reservoir where the top product is collected, the top product is collected during the hot half-cycle. In the cold half-cycle, the feed flows downwards and the bottom product is withdrawn. The end of each half-cycle is set by the time at which all the solution contained in one reservoir is completely transferred to the other reservoir. Temperatures are 60°C at the bottom of the column and 18°C at the top of the bed for the phenol/adsorbent resin Duolite ES861 system; for the phenylalanine/adsorbent resin SP206 system, hot and cold temperatures are 40 and 15°C, respectively.

The separation potential of thermal parametric pumping can be assessed by using the parameter b, introduced by Pigford et al. [21] and defined as $b = a/(1 + \bar{m})$, where $\bar{m} = (m(T_1) + m(T_2))/2$ is the average of the capacity factors at the cold and hot temperatures, T_1 and T_2, respectively, $a = (m(T_1) - m(T_2))/2$ and $m(T) = ((1-\varepsilon)/\varepsilon)\rho_{ap} K(T)$ is the capacity parameter for a linear adsorption equilibrium isotherm with slope $K(T)$. Table 1 reports values of the separation parameter b for some systems studied by parametric pumping.

Various examples of parametric pumping operations at laboratory scale have been published [5,23,24,25]. Batch, semi-continuous and continuous modes of operation have also been addressed [2,3,4].

The modeling of parametric pumping processes has been dealt with by various researchers. Pigford et al. [21] first used the equilibrium model to analyze parametric pumping adsorptive processes with linear equilibrium isotherms; Gregory and Sweed [11] applied that model to various pro-

* Corresponding author. Fax: +351-2-319280.

[1] Present address: Chemical Engineering Department, Faculty of Sciences and Technology, University of Coimbra, 3000 Coimbra Codex, Portugal.

1385-8947/00/$ – see front matter
PII: S1385-8947(99)00117-5

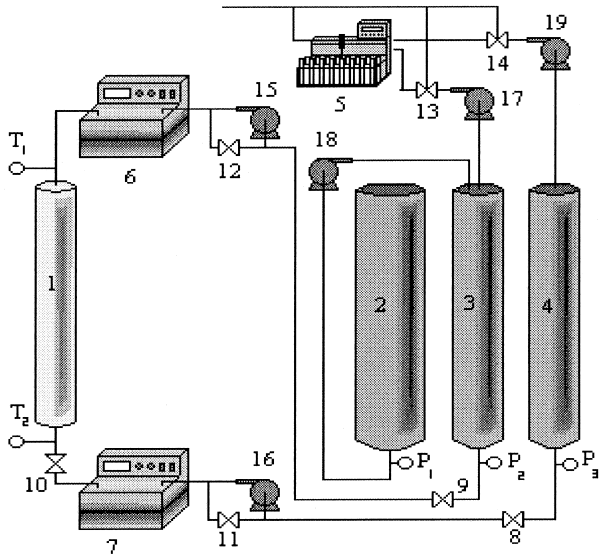

Fig. 1. Experimental setup. 1 Glass column; 2 feed reservoir; 3 top reservoir; 4 bottom reservoir; 5 fraction collector; 6–7 heat exchangers; 8–12 two-way solenoid valves; 13–14 three-way solenoid valves; 15–19 peristaltic pumps; T_1–T_2 thermocouples; and P_1–P_3 pressure transducers.

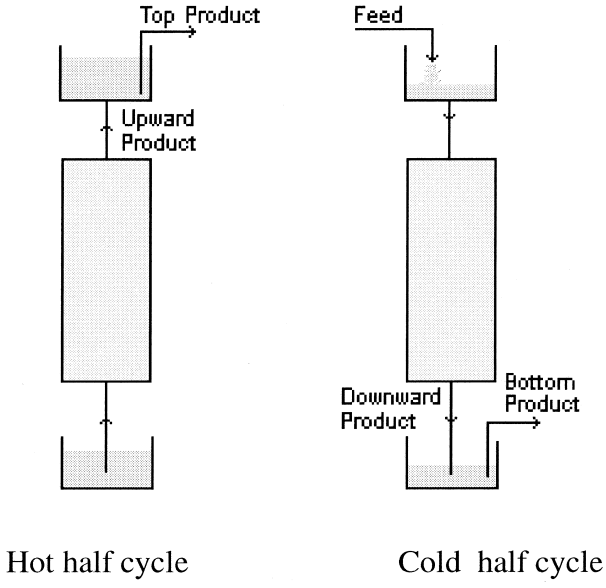

Fig. 2. Semi-continuous operation of parametric pumping.

cess configurations. Equilibrium staged models were used by Grevillot and Tondeur [12,13,14]. Mass-transfer rate was included in the works of Sweed and Wilhelm [27] and Gupta and Sweed [15].

Recently, Ferreira and Rodrigues [8] developed a more complete model accounting for axial dispersion in the fluid phase, film mass transfer, intraparticle mass transfer and heat transfer through the wall. The model also assumed perfectly mixed reservoirs. The model successfully predicts the behavior of thermal parametric processes, such as phenol purification with polymeric adsorbent Duolite ES861 [9] and phenylalanine adsorption in polymeric adsorbent SP206 [8].

Table 1
Separation factor b for several systems

System	T_{cold} (°C)	T_{hot} (°C)	b	Reference
Phenol/Duolite ES861	20	60	0.20–0.37	[8,9]
Phenylalanine/SP206	15	40	0.40	[7]
n-Heptane–toluene/silica gel	4	70	0.125	[30]
n-Heptane–toluene/silica gel	15	70	0.083	[30]

Table 2
Dimensionless equations for Model I (equilibrium + axial dispersion)

Mass balance in a volume element of the column

$$\frac{1}{Pe}\frac{\partial^2 X}{\partial z^{*2}} \pm \frac{\partial X}{\partial z^*} = (1+\nu)\frac{\partial X}{\partial \theta} + \xi_m \frac{\partial Y}{\partial \theta}$$

Energy balance in the column

$$\frac{1}{Pe_h}\frac{\partial^2 T^*}{\partial z^{*2}} \pm \frac{\partial T^*}{\partial z^*} - N_{hw}(T^* - T^*_{amb}) = (1+\xi_h)\frac{\partial T^*}{\partial \theta}$$

Adsorption equilibrium isotherm

$$Y^* = \frac{K_L X_p}{1+K_L X_p}$$

with $K_L = k_0 C_E \exp\left(\frac{\gamma}{T^*}\right)$ and $\gamma = \frac{-\Delta H}{RT_{ref}}$

However, in cyclic processes with long cycle times, i.e., $(D_{pe}t_c/R_p^2) > 0.1$, the model can be simplified since intraparticle mass transfer can be described by the linear driving force (LDF) approximation. This is not the case in fast cyclic adsorption/desorption processes [1].

The objectives of this work are:

1. the analysis of thermal parametric pumping processes by two simplified models: model I based on equilibrium and axial dispersion, and model II based on linear driving force (LDF) approximation for intraparticle mass transfer and axial dispersion;
2. the test of model validity by comparison with experiments in a pilot plant for the system phenylalanine/water/polymeric adsorbent SP206 and with experimental results from Ferreira and Rodrigues [9] for the system phenol/water/adsorbent resin Duolite ES861; and
3. the development of a user-friendly package of thermal parametric pumping for educational and training purposes.

2. Modeling of thermal parametric pumping processes

The two simplified models to be developed here are: Model I, which considers equilibrium between fluid and adsorbent particles and axial dispersion in the fluid phase; and Model II, which uses the linear driving force (LDF) approximation to describe intraparticle mass transfer and also includes axial dispersion in the fluid phase. The energy balance for the system is considered in both models.

Dimensionless equations for Model I (equilibrium plus axial dispersion) shown in Table 2 are:

1. mass balance in a volume element of the fluid phase;
2. energy balance;
3. kinetic law for intraparticle mass transfer; and
4. adsorption equilibrium isotherm.

Table 3
Dimensionless equations for Model II (LDF)

Mass balance in a volume element of the column

$$\frac{1}{Pe}\frac{\partial^2 X}{\partial z^{*2}} \pm \frac{\partial X}{\partial z^*} = \frac{\partial X}{\partial \theta} + \xi_m \frac{\partial \langle Y\rangle}{\partial \theta} + \nu \frac{\partial \langle X_p\rangle}{\partial \theta}$$

Energy balance in the column

$$\frac{1}{Pe_h}\frac{\partial^2 T^*}{\partial z^{*2}} \pm \frac{\partial T^*}{\partial z^*} - N_{hw}(T^* - T^*_{amb}) = (1+\xi_h)\frac{\partial T^*}{\partial \theta}$$

Mass balance inside particles

$$\xi_m \frac{\partial \langle Y\rangle}{\partial \theta} + \nu \frac{\partial \langle X_p\rangle}{\partial \theta} = N_p\left(X - \langle X_p\rangle\right)$$

Adsorption equilibrium isotherm

$$Y^* = \frac{K_L X_P}{1+\tilde{K}_L X_P}$$

with $\tilde{K}_L = k_0 C_E \exp\left(\frac{\gamma}{T^*}\right)$ and $\gamma = \frac{-\Delta H}{R\,T_{ref}}$

In the model equations, $X = C/C_E$ is the dimensionless solute concentration in the bulk fluid phase, $Y = q/Q_\infty$ the dimensionless adsorbed phase concentration, $T^* = T/T_{ref}$ the dimensionless temperature in the bulk fluid phase, $z^* = z/L$ the dimensionless axial coordinate and $\Theta = t/\tau$ the reduced time variable. In the equilibrium model, the dimensionless solute concentration in the bulk fluid phase, X, is equal to the dimensionless solute concentration in the fluid inside the pores $X_p = C/C_P$.

Model parameters for the equilibrium + axial dispersion model are:

Axial dispersion parameters:

Mass Peclet number $Pe = \frac{u\,L}{\varepsilon\,D_{ax}}$

Heat Peclet number $Pe = \frac{u\,L}{K_{æ}/\rho_f C_{pf}}$

Capacity parameters:

Mass capacity factor: $\xi_m = \frac{1-\varepsilon}{\varepsilon}\frac{\rho_h f_h q_e}{C_e}$

Thermal capacity factor: $\xi_h = \frac{1-\varepsilon}{\varepsilon}\frac{\rho_s C_{ps}}{\rho_f C_{pf}}$

Adsorption equilibrium parameters:

Nonlinearity of the isotherm: $K_L = k_0 \exp\left(\frac{-\Delta H}{RT^* T_{ref}}\right)$

Arrhenius number: $\gamma = \frac{-\Delta H}{RT_{ref}}$

Geometrical parameter:

Intraparticle pore volume/interparticle void volume ratio: $\nu = \frac{1-\varepsilon}{\varepsilon}\varepsilon_p$

Heat transfer parameter:

Number of wall heat transfer units: $N_{hw} = \frac{h_{we} a_w \tau}{\rho_f C_{pf} \varepsilon}$

Model II is a nonisothermal, nonadiabatic model which takes into account the mass-transfer resistance inside the particle. The intraparticle mass-transfer rate is described by the linear driving force (LDF) approximation [10]. The model contains one more parameter related with intraparticle mass transfer, i.e. $N_P = ((1-\varepsilon)/\varepsilon)\,K_P\,\tau$, where $K_P = 15 D_{pe}/R_p^2$ is the rate constant for intraparticle mass transfer.

Table 3 shows dimensionless equations for Model II (LDF — linear driving force approximation). Model II contains one additional equation for the kinetics of mass transfer inside the adsorbent particle. In addition to the dimensionless variables already defined in Model I, (equilibrium + axial dispersion), the average solute concentration in fluid inside pores $\langle X_p\rangle$ and in adsorbed phase $\langle Y\rangle$ have to be included in Model II.

Table 4
External balances (reservoirs), boundary and initial conditions for LDF and equilibrium models

External balances (reservoirs):			
Hot half-cycle:	$\langle X_{BP}\rangle_n = \langle X_{BP}\rangle_{n-1}$		
	$< X_{TP} >_n = \frac{(1-\phi_B)< X(1,\theta)>_n}{1+\phi_T} + \frac{\phi_B+\phi_T}{1+\phi_T}$		
Cold half-cycle:	$\langle X_{BP}\rangle_n = \langle X(0,\theta)\rangle_n$		
Boundary conditions:			
Hot half-cycle:	$z^* = 0$	$X(0,\theta) = \langle X_{BP}\rangle_n$	$T^* = T_{hf}/T_{ref}$
	$z^* = 1$	$\partial X(z^*,\theta)/\partial z^* = 0$	$\partial T^*(z^*,\theta)/\partial z^* = 0$
Cold half-cycle:	$z^* = 0$	$\partial X(z^*,\theta)/\partial z^* = 0$	$\partial T^*(z^*,\theta)/\partial z^* = 0$
	$z^* = 1$	$X(1,\theta) = \langle X_{TP}\rangle_n$	$T^* = T_{cf}/T_{ref}$
Initial conditions	$\theta = 0$	$X(z^*,0) = 1$	$T^*(z^*,0) = T_0/T_{ref}$

The adsorption equilibrium is established at each point of the pore/solid interface between the fluid pore concentration X_p and the adsorbed phase concentration $Y^* = Y$. The adsorption equilibrium isotherm considered here is of the Langmuir type, i.e. $q^* = Q_\infty K_L C_p/\{1 + K_L C_p\}$ or in dimensionless terms $Y^* = \tilde{K}_L X_p/\{1 + \tilde{K}_L X_p\}$, where $\tilde{K}_L = K_L C_E$.

The external balances (reservoirs), boundary and initial conditions for equilibrium and LDF models are provided in Table 4. The boundary conditions are established for each half-cycle at both extremities of the adsorption column. In the upward hot half-cycle, the entering condition is determined by the external balance in the bottom reservoir; similarly, in the downward cold half-cycle, the entering condition results from the external balance in the top reservoir. In both half-cycles the boundary condition on the exit side of the column is of Danckwerts type.

3. Numerical solution

The system of PDEs presented is solved by the method of the lines [22], using orthogonal collocation in finite elements OCFE for the spatial coordinate. The spatial coordinate is discretized based on the evaluation of the set of differential equations written in its residual form and evaluating them in the characteristics roots of a family of orthogonal Gauss–Legendre polynomials. This method is implemented in a numerical package called PDECOL by Sincovec and Madsen [26] and Madsen and Sincovec [19], introducing B-splines polynomials [6] as base functions over the spatial integration domain. The PDECOL package is written in Fortran and has been used successfully in the simulation of the adsorption/convection process for a slab particle, cyclic adsorption processes as pressure swing adsorption (PSA), pressure swing adsorptive reactors [17,18] and more recently in the dynamic simulation of a simulated moving bed adsorber [20]. PDECOL solves systems of partial differential equations with the structure $\partial\vec{B}/\partial\theta = \vec{f}(\theta, z*, \vec{B}, \partial\vec{B}/\partial z*, \partial^2\vec{B}/\partial z*^2)$, where $\vec{B}$ is a column vector containing the dependent variables. The dependent variables in the equilibrium model are X and T^*, while in the LDF model, they are X, $\langle X_p\rangle$ and T^*. The $\vec{f}$ column vector results from solving the differential equation for the time

derivative. Once the equations are structured as described above, they are introduced in a wrapper routine 'F', which is called by pdecol. When 'F' subroutine is called, pdecol provides the values of X, T^* and the first and second spatial derivatives of these variables and then $\vec{f}$ is computed. The advance in time is performed using backward difference formulas, through gearib-type algorithm [16] which is convenient for solving stiff ODE systems. This ODE solver is included in the PDECOL package and exploits the band structure obtained during the discretization of the system of equations, when the B-spline polynomials are introduced. The system of equations is completed with the introduction of the initial and boundary conditions. The initial conditions are written in the UINIT subroutine, where X and T^* are defined at each point z^* from 0 to 1, at $\theta = 0$. The boundary conditions are defined in the subroutine BNDRY, such that the initial and boundary conditions are consistent at $\theta = 0$. Pdecol offers a flexible interpolating routine called VALUES, where computed results after each interval of time advanced are obtained.

The number of equations, N, to be solved is *NPDE*NCPTS* where *NPDE* is the number of partial derivatives, and *NCPTS* the number of collocation points. The number of the collocations points is $KORD*NINT - NCC*(NINT - 1)$, where *NINT* is the number of elements, *KORD* the polynomial degree +1 and *NCC* the number of continuity conditions between adjacent elements to be satisfied by the B-spline basis. In this work, the recommended values of $KORD = 1$and $NCC = 2$ were selected, so that $N = 2*NPDE*(NINT + 1)$. For example, selecting 20 elements for the spatial coordinate, the total number of equations to be solved are 84 in the equilibrium model ($NPDE = 2$), while for the LDF model ($NPDE = 3$) 126 equations are solved.

4. Simulation results

In this section, the effect of the dispersive parameters, mass Peclet number, *Pe*, and number of intraparticle mass transfer units, N_p, on the separation performance will be studied. The simulations were based on parameter values given in Table 5 for the system phenol/water/adsorbent resin Duolite ES 861 [8].

4.1. Effect of the mass Peclet number on the separation performance

The effect of mass Peclet number, *Pe*, on the process performance is shown in Fig. 3 for the equilibrium + axial dispersion model (Model I) and in Fig. 4 for the LDF model (Model II). In both cases, as the axial dispersion increases, the Peclet number is reduced, and so is the separation performance. For Model I, the results from the limiting equilibrium model are obtained for $Pe > 120$.

The values of the mass Peclet number were 20, 50 and 120 for both models, and also $Pe = 200$ for the LDF model (Model II).The column used was 0.75 m long and the total cycle time was 5.6 h.

Table 5
Parameter values used for the simulation of semicontinuous parametric pumping in recuperative mode: system phenol/water/adsorbent resin Duolite ES861 (from Ref. [8])

Characteristics of the resin:	*Model parameters*:
ρ_h (kg wet resin/m^{3}wet resin) = 1020	$Pe = 120$
$f_H = 0.28$ kg dry resin/kg wet resin	$Pe_h = 100$
R_p ($\times 10^4$ m) = 2.35	*Bed characteristics*:
$\epsilon_P = 0.72$	L (m) = 0.75
$\tau_P = 2.93$	d (m) = 0.09
$\xi_h = 1.3$	$\epsilon = 0.40$
Operating variables:	*Transport parameters*:
T_{cf} (K) = 293	D_{mcc} (m^2/s) = 8.9×10^{-10}
T_{hf} (K) = 333	D_{mhc} (m^2/s) = 2.2×10^{9}
T_{ref} (K) = 273	h_{we} (kJ/m^2 K s) = 1.42×10^{-2}
V_U (m^3) = 0.0236	$N_{hwhc} = 0.22$
$Q\pi/\omega$ (m^3) = 0.0324	$N_{hwcc} = 0.29$
$\phi_B = 0.27$	*Equilibrium parameters*:
$\phi_T = 0.14$	Q_∞ (kg solute/kg dry resin) = 0.07
t_{hc} (min) = 118	k_0 (m^3 solution/kg solute) = 3.96×10^{-4}
t_{cc} (min) = 218	ΔH (kJ/kmol) = −22751
Q_{hc} (m^3/s) = 3.33×10^{-6}	
Q_{cc} (m^3/s) = 2.50×10^{-6}	
Q_{feed} (m^3/s) = 1.88×10^{-6}	
Q_{BP}(m^3/s) = 6.60×10^{-7}	
Q_{TP}(m^3/s) = 6.40×10^{-7}	
$C_E = 0.099$ kg solute/m^3 solution	

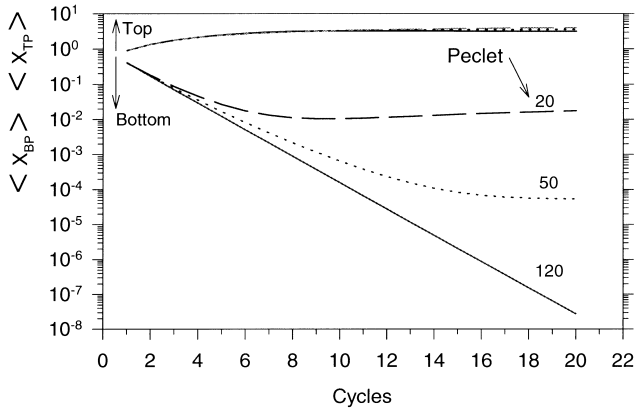

Fig. 3. Effect of mass Peclet number on the separation by semicontinuous, recuperative mode, parametric pumping. Simulations based on the equilibrium plus axial dispersion model (Model I) for the system phenol/adsorbent resin Duolite ES 861.

4.2. Effect of the intraparticle mass-transfer coefficient, K_P

In the linear driving force approximation, the mass transfer rate is assumed to be proportional to the driving force given by the difference between the fluid phase concentration at the particle surface and the average solute concentration inside pores. The intraparticle mass transfer coefficient is inversely proportional to R_p^2. Smaller particles will, there-

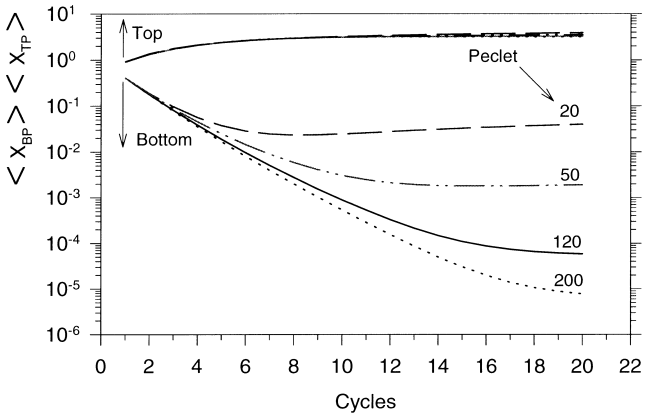

Fig. 4. Effect of mass Peclet number on the concentration (top and bottom) vs. cycle number in semicontinuous parametric pumping in recuperative mode. Simulations based on the LDF model (Model II) for the system phenol/adsorbent resin Duolite ES 861.

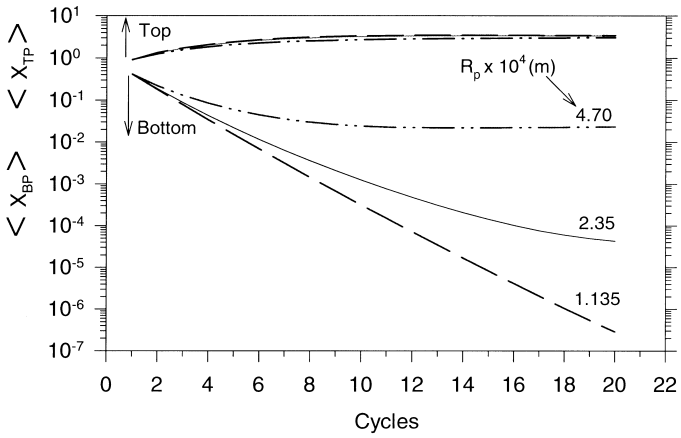

Fig. 5. Effect of particle size on the concentration (top and bottom) vs. cycle number in semicontinuous parametric pumping in recuperative mode. Simulations based on LDF model (Model II) for the system phenol/adsorbent resin Duolite ES 861.

Table 6
Values of K_p and N_{hw} parameters used in the simulations to study the effect of particle radius

R_p ($\times 10^4$m)	K_{phc} (min^{-1})	K_{pcc} (min^{-1})	N_{hw} hc	N_{hw} cc
1.175	35.24	14.26	0.25	0.33
2.35	8.81	3.56	0.25	0.33
4.70	2.20	0.89	0.25	0.33

fore, lead to better separations as shown in Fig. 5. It can be seen that, for particles of around 100 μm, mass-transfer resistance can be neglected and then results can be predicted by the equilibrium theory.

In Table 6, the values of parameters K_p and N_{hw} which were kept constant during each half-cycle are shown. The bed length used in the simulations was 0.85 m.

5. Package description

The graphic user interface (GUI) was developed in Visual Basic language, version 4.0 which is a fast and reliable developing platform in Windows environment [28]. The user-friendly GUI supported by the Visual Basic facilities allows a fast learning curve of the new package, making easy the understanding of the parametric pumping process, and therefore it is a powerful training and teaching tool.

5.1. Package development

The new package called Visual Pumping (VP) is the result of linking two main sources. The library PDECOL compiled in Fortran language and the main program compiled in Visual Basic within the GUI is controlled, and the communication between the GUI and the PDECOL solver is guaranteed. The block diagram of VP is shown in Fig. 6. The main program is constituted by a main event handler routine, which intercepts any change over the GUI generated by the user (as keystrokes, mouse movements, menu selection requests). The main program records the specifications of the simulating case and then, when the input data is completed, it is sent to PDECOL engine. Once the numerical integration is carried out, the results are shown back in the GUI.

The Main Program is written in Visual Basic and works as a manager of events. The link between Fortran and Visual Basic codes is as follows:

1. the program in Visual Basic reads the Initial Data needed to execute the Fortran program and calls the Fortran program with user's options;
2. the Fortran program reads the data generated by the Visual Basic and calls the PDECOL subroutines;
3. during the cycle time chosen, PDECOL solves model equations given by subroutine integration, Subroutine F, with initial conditions defined in subroutine UINIT, and boundary conditions given by subroutine BNDRY;
4. Fortran calls the subroutine VALUES, which gives the bed axial position, the solute concentration in pores, the solute concentration in the bulk fluid , and the bed temperature at given time intervals;
5. the Fortran program stores the values generated at each half-cycle;
6. the Visual Basic program reads the temporal archives generated by the Fortran program; and
7. the Visual Basic draws a graph showing the evolution of the average solute concentration in the fluid phase in the top and bottom of the bed, indicates in which half-cycle the simulation is taking place and displays the graphs for temperature and concentration profiles.

5.2. Install procedure

The Install procedure of Visual Pumping, version 1.0, is straightforward, while the user follows the directions after

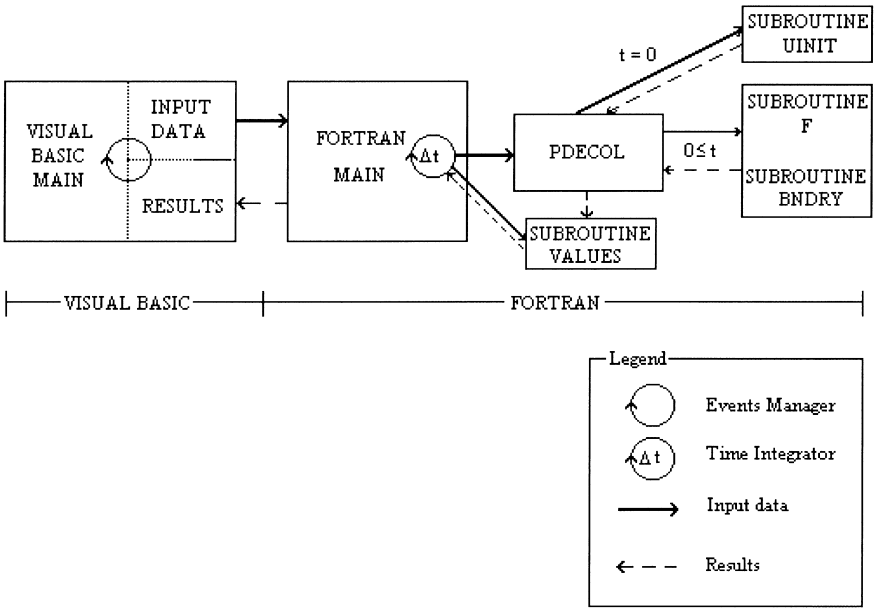

Fig. 6. Block diagram.

run the 'setup.exe' program. The main frame contains the options to be made: choice of the model, process objective, parameter values and data base, with experimental values or not. The simulator *Visual Pumping 1.0*: provides the following options:

5.2.1. Select the database for the simulation

Two solutes, phenol or phenylalanine, can be chosen for the simulation. For each solute there is a data base with all parameters, which can be seen in the menu 'Initial Values', which has also the numerical parameters to be used in PDECOL.

The system selected was phenol/water/adsorbent resin Duolite ES861 with the objective of bottom product purification.

5.2.2. Menu 'Initial Values'

'Parameters' — shows the value of the following parameters
'Resin and Bed Characteristics' Variables'
'Models Parameters'
'Mathematical Constants; — shows the numerical parameters for PDECOL.

To change a parameter, the cursor should be directed to the area with the value of that parameter. After each simulation the initial values of the parameters, even if they were changed, return to the pre-set values. Therefore, if the user carries various simulations he has to enter data for the problem as many times as needed.

5.2.3. Experimental data

Simulation results are compared with experimental data obtained for each case. In this case, it is convenient to simulate with data stored in the program. *Select this option if you want to provide your own data*. If experimental data are different from those stored, one should choose the option for providing experimental data and change parameters in the model.

5.2.4. Number of cycles

The user can choose the number of cycles to be used in the simulation. When comparing with experimental data the program indicates in the screen the number of cycles used in the experiment.

5.2.5. Model

Defines the models for the simulation. The Menu 'Models' allows the choice of the

Menu 'Models':
'Equilibrium with Axial Dispersion Model Equations'
'Linear Driving Force with Axial Dispersion Model Equations'
'General Equations' — reservoirs, boundary and initial conditions.

5.2.6. Process objective

The user can define the objective: purify the bottom product or concentrate the top product.

5.2.7. Go

When the user is sure that all data are correctly inserted to run the program, the user selects the model within the menu 'Models' and then the button 'Executar' is available.

Fig. 7 shows the screen in which the process evolution is displayed, with the graphs of top and bottom product concentration of phenol vs. time of operation as well as the

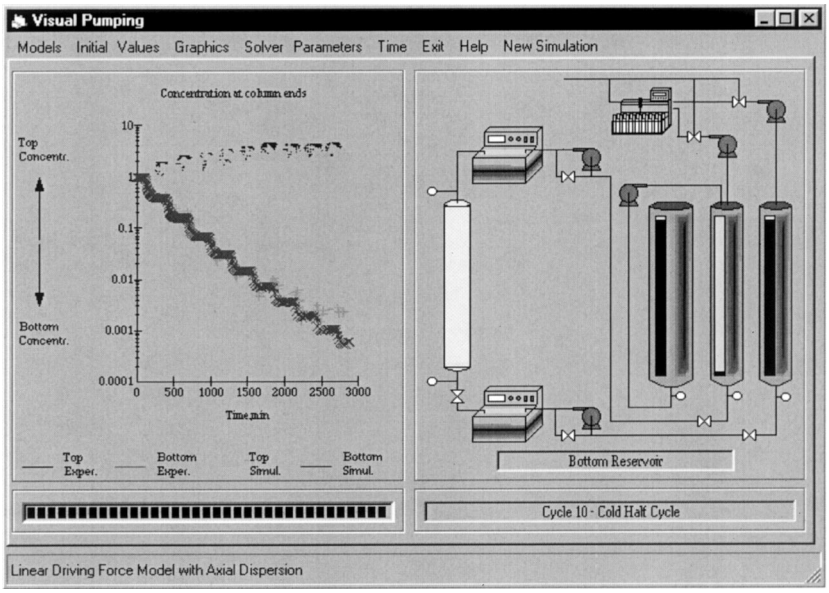

Fig. 7. Screen of the program under execution.

scheme of the equipment. The number of the cycle and type of half-cycle is also shown. At the end of the simulation, results data are read as indicated by the bar informing of the progress of that action. Simulated results with Model II are compared with experimental data.

5.2.8. Menu 'Graphics'

It allows the user to construct graphs for cycles 1, 2, 5, 10, 15 or 20, for solute concentration in the liquid phase, adsorbed phase as well axial temperature profiles at various times.

Fig. 8 shows graphs for cycle 10 by choosing in the 'Graphs' the option 'cycle 10'. At cyclic steady state, the axial concentration profiles (in the fluid phase and in the adsorbed phase) are stabilized inside the column between two limiting lines at the start and end of a cycle; this is characteristic of flow reversal systems. Since the thermal wave travels much faster than the concentration wave, the bed temperature changes more rapidly than the concentration changes in the bed. The axial temperature profiles in the hot half-cycle, where the feed enters from the bottom ($z^* = 0$) at 60°C, are shown at time $t =$ 1; 11; 21 ; 31 ;51; 71; and 101 min (end of the hot half-cycle). The last four lines are almost superimposed; the bed at 31 min is at the hot temperature. In the cold half-cycle, the feed enters at the top of the bed ($z^* = 1$) at 18°C; temperature profiles from the right to the left are shown at $t = 1$; 11, 21; 31; 71; 101; 151 and 181 min (end of cold half-cycle) and again the bed is at the cold temperature after 31 min. In the simulation values of operating variables for this run were: $V_U = 0.03132\,m^3$, $Q\pi/w = 0.03982\,m^3$, $\phi_B = 0.22$, $\phi_T = 0.11$, $Q_{hc} = 4.83 \times 10^{-6}\,m^3/s$, $Q_{cc} = 3.67 \times 10^{-6}\,m^3/s$, $Q_{feed} = 1.188 \times 10^{-6}\,m^3/s$, $Q_{BP} = 1.31 \times 10^{-6}\,m^3/s$, $Q_{TP} = 4.1 \times 0^{-6}\,m^3/s$ and $C_E = 0.096$ kg solute/m^3 solution.

5.2.9. Solver parameter

It shows the model parameters used in the simulation.

5.2.10. Time

Indicates the time of simulation.

6. Experimental example and test of the models

The experimental set-up for the study of thermal adsorptive parametric pumping in recuperative mode is shown in Fig. 1. It contains four main sections: column and ancillary equipment, reservoirs, sample collection and analysis and automation section. The column is an Amicon G90 × 1000 column of 9-cm diameter. The packing was the adsorbent resin SP-206 with average diameter of 400 mm (Mitsubishi, Japan). Peristaltic pumps (Watson–Marlow) were used to circulate the solution downward at 15°C and upward at 40°C.

The 0.001 M solution of phenylalanine was prepared by dissolving the solid in a 0.01 M phosphate buffer (KH_2PO_4 with pH 6.5 adjusted with NaOH).

The column with length of 0.85 m was equilibrated at the cold temperature with the feed solution and the cycle started with the hot half-cycle by flowing the solution upward at 40°C. The top product is collected and the aminoacid concentration analyzed by UV spectrometry at 275.2 nm. Then the cold half-cycle starts with feed at the top and collection of the bottom product. The cyclic steady state is reached after 1000 min, but after five cycles we are very close to the cyclic regime.

Experimental results are shown in Fig. 9 for the top and bottom concentrations as functions of time. The predictions of equilibrium + axial dispersion model (Model I . . .) and LDF model (Model II _ _) are also shown. The parameters

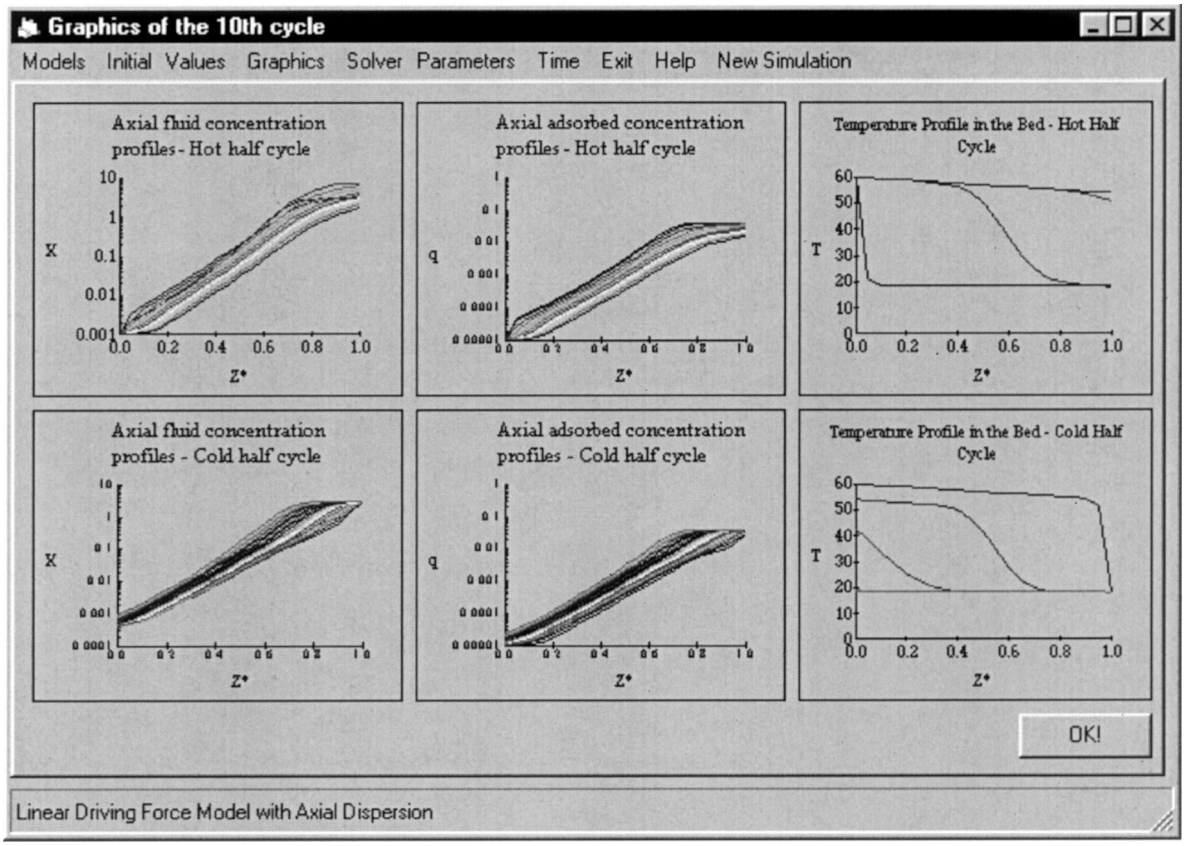

Fig. 8. Screen with graphs for cycle 10.

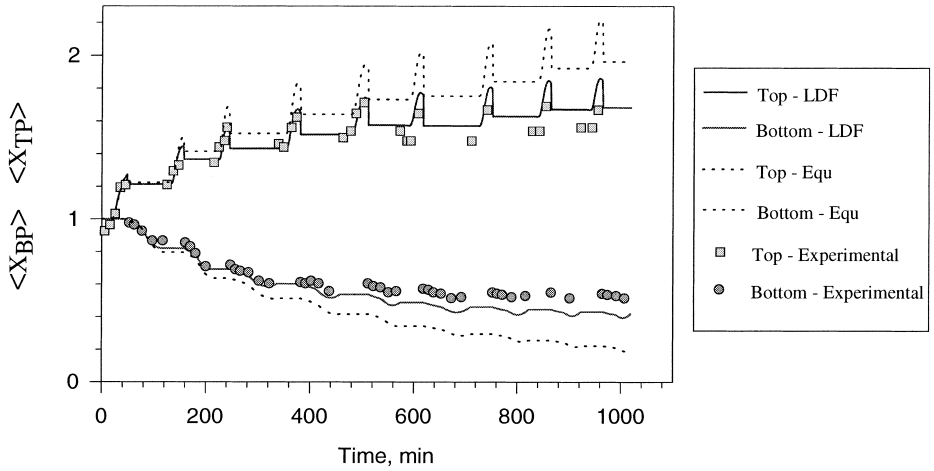

Fig. 9. Experimental results and model predictions: (—) LDF model; equilibrium + axial dispersion model) for the system phenylalanine/water/adsorbent resin SP-206.

used in the experiment are reported in Table 7. It can be seen that Model II predictions are in good agreement with experimental results; therefore, the linear driving force approximation used in Model II is adequate to describe intraparticle mass transfer in cyclic processes with long cycle times.

The validity of LDF model (Model II) was also tested by using experimental data for the system phenol/water/adsorbent resin Duolite ES861 reported by Ferreira and Rodrigues [9] and shown in Fig. 10. Those authors used a more complete model in which diffusion equation was included to describe intraparticle mass transfer (model represented by the dotted line in Fig. 10). However, the simplified LDF model presented in this work is sufficiently good in predicting the performance of the

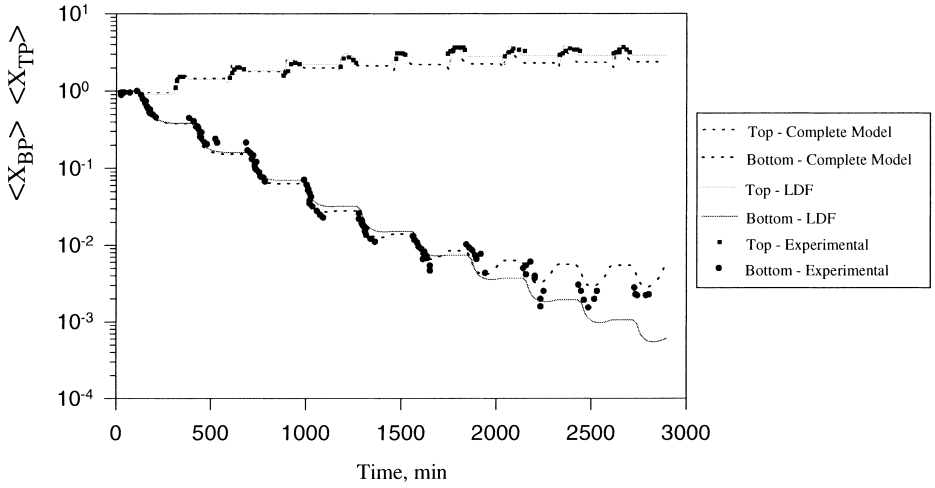

Fig. 10. Experimental results and model predictions (—) LDF model; (...) complete model of Ferreira and Rodrigues [9] for the system phenol/water/adsorbent resin Duolite ES861.

Table 7
Parameter values used in the simulation of semicontinuous parametric pumping in recuperative mode : system phenylalanine/water/adsorbent resin SP-206 (Díez et al. [7])

Characteristics of the resin:	*Model parameters*:
ρ_h(kg wet resin /m^3wet resin) = 1190	Pe = 120
f_H = 0.50 kg dry resin/kg wet resin	Pe_h = 80
R_p ($\times 10^4$ m) = 2.00	*Bed characteristics*:
ϵ_P = 0.6069	L (m) = 0.85
τ_P = 2.00	d (m) = 0.09
ξ_h = 1.205	ϵ = 0.40
Operating variables:	*Transport parameters*:
$T_{coldfeed}$ (K) = 288	D_{mcc} (m^2/s) = 5.8×10^{-10}
$T_{hotfeed}$(K) = 313	D_{mhc} (m^2/s) = 1.1×10^{-9}
T_{amb} (K) = 288	D_{pecc} (m^2/s) = 1.76×10^{-10}
T_{ref} (K) = 273	D_{pehc} (m^2/s) = 3.34×10^{-10}
V_U (m^3) = 0.009675	h_{we} (kJ/m^2 K s) = 1.42×10^{-2}
$Q\pi/\omega$ (m^3) = 0.01106	K_{phc} (min^{-1}) = 7.51
ϕ_B = 0.147	K_{pcc} (min^{-1}) = 3.96
ϕ_T = 0.089	N_{hwhc} = 0.218
t_{hc} (min) = 43	N_{hwcc} = 0.310
t_{cc} (min) = 70	*Equilibrium parameters*:
$Q_{hc} \times 10^6$(m^3/s) = 3.75	Q_∞ (kg solute/kg dry resin) = 0.066
$Q_{cc} \times 10^6$(m^3/s) = 2.65	k_0 (m^3 solution/kg solute) = 3.96×10^{-4}
$Q_{feed} \times 10^7$ (m^3/s) = 5.42	ΔH (kJ/kmol) = −14698
$Q_{BP} \times 10^7$ (m^3/s) = 3.33	
$Q_{TP} \times 10^7$ (m^3/s) = 3.33	
C_E = 0.1652 kg solute/m^3 solution	

parametric pumping unit as shown by the full line in Fig. 10.

7. Conclusions

A user-friendly package written in Visual Basic was developed for the simulation of parametric pumping adsorptive processes as a tool for educational and training purposes.

Two models were implemented in the package: Model I is the equilibrium + axial dispersion model; Model II is a linear driving force (LDF) model with axial dispersion, which is a convenient tool for the analysis of cyclic processes with long cycle times, such as parametric pumping.

Simulated results from this simplified Model II are similar to those obtained with more sophisticated models involving PDE for intraparticle diffusion and require much lower computing time. The LDF model was validated experimentally in the pilot plant existing at the LSRE, University of Porto, for the system phenylalanine/water/polymeric adsorbent SP206 and using results from Ferreira and Rodrigues (1995b) for the system phenol/water/Duolite ES861.

8. Nomenclature

a_w	specific area of wall ($4/d$) (m^{-1})
A	column section area (m^2)
C	solute concentration in the fluid phase (Kg/m^3)
C_E	feed solute concentration (Kg/m^3)
$\langle C_P \rangle$	average solute concentration in the pores (Kg solute/m^3 fluid in the pores)
C_P	solute concentration in the pores (Kg solute/m^3 fluid in the pores)
C_{pf}	heat capacity of the fluid (kJ/Kg K)
C_{PS}	solute concentration in the pores at particle surface (Kg solute/m^3 fluid in the pores)
C_s	heat capacity of the adsorbent (kJ/Kg K)
d	column diameter (m)
D_{ax}	axial dispersion coefficient (m^2/s)
D_m	molecular diffusion coefficient (m^2/s)
D_{pe}	pore effective diffusivity (m^2/s)
d_p	particle diameter (m)
f_H	humidity factor for the adsorbent (kg dry resin/kg wet resin)

h_{we}	wall heat transfer coefficient (kJ/(m^{2}sK)
ΔH	heat of adsorption (kJ/kmol)
$K(T)$	slope of linear isotherm
K_{ae}	axial thermal conductivity (kJ/msK)
K_l	parameter of the Langmuir isotherm (m^{3}solution/Kg solute)
$\tilde{K}_l$	Langmuir parameter (=$K_l C_E$)
K_P	linear driving force constant (s^{-1})
k_0	parameter of the modified Langmuir isotherm (m^3 solution/Kg solute)
l	bed height (m)
$m(T)$	mass capacity parameter
n	number of cycles
N_p	number of mass transfer units for pore diffusion
N_{hw}	number of wall heat transfer units
Pe	mass Peclet number
Pe_h	thermal Peclet number
q	adsorbed solute concentration (Kg solute/Kg dry resin)
q^*	adsorbed solute concentration in equilibrium with the concentration of solute in the fluid phase (Kg solute adsorbed/Kg dry resin)
$\langle q \rangle$	average adsorbed solute concentration (Kg adsorbed solute/Kg dry resin)
q'_E	adsorbed solute concentration in equilibrium with the feed concentration (Kg adsorbed solute/m^3 wet resin)
Q	flow rate (m^3/s)
Q_∞	maximum adsorbent capacity (Kg solute/Kg dry resin)
$Q(\pi/\omega)$	reservoir displacement volume (m^3)
r	radial coordinate (m)
R	ideal gas constant (kJ/(kmol K)
R_p	particle radius (m)
t	time (s)
t_c	cycle time (s)
t_{cc}	cold half-cycle time (s)
t_{hc}	hot half-cycle time (s)
t_{ST}	stoichiometric time (s)
T	temperature (K)
T_{amb}	ambient temperature (K)
T_{cc}	cold temperature (K)
T_{hc}	hot temperature (K)
T_{ref}	reference temperature (K)
T^*	normalized temperature
u	superficial velocity (m/s)
u_{cn}	concentration wave velocity (m/s)
u_i	interstitial velocity (m/s)
u_{th}	thermal wave velocity (m/s)
V_U	volume percolated in upward flow (m^3)
X	normalized fluid phase concentration
X_P	normalized fluid concentration in the pores
Y	normalized adsorbed phase concentration (=q/Q_∞)
z	spatial coordinate (m)
z^*	normalized axial coordinate

8.1. Greek letters

ξ_m	mass capacity parameter
ξ_h	thermal capacity parameter
ϵ	bed porosity
ϵ_P	intraparticle porosity
ϕ_B	fraction of the $Q(\pi/\omega)$ withdrawn as bottom product
ϕ_T	fraction of the $Q(\pi/\omega)$withdrawn as top product
ρ_f	density of the fluid (Kg solution /m^3 solution)
ρ_h	wet density of the adsorbent (Kg wet resin/m^3 wet resin)
ρ_s	density of the adsorbent (Kg dry resin/m^3 dry resin) ($\rho_s = \rho_h f_H$)
θ	time normalized by the space time
θ^*	time normalized by the stoichiometric time
τ	space time (s)
τ_P	tortuosity factor
ν	intraparticle pore volume/interparticle void volume ratio
ω	frequency of temperature change (s^{-1})
(π/ω)	duration of half cycle (s)

8.2. Subscripts

E	entrance
BP	bottom product
TP	top product
cc	cold half-cycle
hc	hot half-cycle
0	initial

References

[1] E. Alpay, D.M. Scott, The linear driving force model for fast-cycle adsorption and desorption in spherical particles, Chem. Eng. Sci. 47(2) (1992) 499–502.
[2] H. Chen, F. Hill, Characteristics of batch, semicontinuous, and continuous equilibrium parametric pumps, Sep. Sci. Technol. 6 (1971) 411–434.
[3] H. Chen, J. Rak, J. Stokes, F. Hill, Separation via continuous parametric pumping, AIChE J. 18(21) (1972) 356–361.
[4] H. Chen, J. Reiss, J. Stokes, F. Hill, Separation via semicontinuous parametric pumping, AIChE J. 19(31) (1973) 589–595.
[5] C. Costa, A. Rodrigues, G. Grevillot, D. Tondeur, Purification of phenolic wastewater by parametric pumping: non mixed dead volume equilibrium model, AIChE J. 28(1) (1982) 73–85.
[6] C. de Boor, Package for calculating with B-splines, SIAM J Numer. Anal. 14(3) (1977) 441–472.
[7] S. Diez, A. Leitão, L. Ferreira, A. Rodrigues, Adsorption of phenylalanine onto polymeric resins: equilibrium, kinetics, and operation of a parametric pumping unit, Sep. Purif. Technol. 13(1) (1998) 25–36.
[8] L. Ferreira, A. Rodrigues, Adsorptive separation by thermal parametric pumping Part I: Modeling, Adsorptive separation by thermal parametric pumping Part I: Modeling and simulation, Adsorption 1 (1995) 213–231.
[9] L. Ferreira, A. Rodrigues, Adsorptive separation by thermal parametric pumping. Part II: Experimental study of the purification

of aqueous phenolic solutions at pilot scale, Adsorption 1 (1995) 233–252.
[10] E. Glueckauf, Theory of chromatography. Part 10. Formulae for diffusion into spheres, Theory of chromatography, Trans. Faraday Soc. 51 (1955) 1540–1551.
[11] R. Gregory, N. Sweed, I. Analytical solutions, Chem. Eng. J. 1 (1970) 207–216.
[12] G. Grevillot, D. Tondeur, Equilibrium staged parametric pumping I-Single transfer step for half-cycle and total reflux. The analogy with distillation, AIChE J. 22 (1976) 1055–1063.
[13] G. Grevillot, D. Tondeur, Equilibrium staged parametric pumping II-Multiple transfer steps for half-cycle and reservoir staging, AIChE J. 23 (1977) 840–851.
[14] G. Grevillot, D. Tondeur, Equilibrium staged parametric pumping III. Open systems at steady-state. McCabe–Thiele diagrams, AIChE J. 26 (1980) 120–131.
[15] R. Gupta, N. Sweed, Modeling of non-equilibrium effects in parametric pumping, Ind. Eng. Chem. Fund. 12 (1973) 335–341.
[16] A. Hindmarsh, Preliminary documentation of GEARIB. Solution of implicit systems of ODE's with banded Jacobians, Lawrence Livermore Laboratory, UCID-30130, 1976.
[17] Z.P. Lu, J.M. Loureiro, A.E. Rodrigues, M.D. Le Van, Simulation of a three-step one-column pressure swing adsorption process, AIChE J. 39(9) (1993) 1483.
[18] Z.P. Lu, A.E. Rodrigues, Pressure swing adsorption reactors: simulation of three-step one-bed process, AIChE J. 40(7) (1994) 1120.
[19] N. Madsen, R. Sincovec, PDECOL: general collocation software for PDE's, ACM Trans. Math. Software 3 (1979) 326–351.
[20] L.S. Pais, J.M. Loureiro, A.E. Rodrigues, Modeling strategies for enantiomers separation by SMB chromatography, AIChEJ 44(3) (1998) 561–569.
[21] R. Pigford, B. Baker, D. Blum, An equilibrium theory of the parametric pump, Ind. Eng. Chem. Fund. 8 (1969) 144–149.
[22] W.E. Schiesser, The Numerical Method of Lines, Academic Press, USA, 1991.
[23] G. Simon, L. Hanak, G. Grevillot, T. Szania, G. Marton, Preparative scale aminoacid separation by thermal parametric pumping on an ion exchange resin, J. Chromatogr. B. 664 (1995) 17–31.
[24] G. Simon, L. Hanak, G. Grevillot, T. Szania, G. Marton, Aminoacid separation by preparative temperature swing chromatography, J. Chromatogr. A. 732 (1996) 1–15.
[25] G. Simon, L. Hanak, G. Grevillot, T. Szania, G. Marton, Preparative scale separation of aminoacids by using thermal ion exchange parametric pumping, Chem. Eng. Sci. 52 (1997) 467–480.
[26] R. Sincovec, N. Madsen, Software for nonlinear PDE's, ACM Trans. Math. Software 1 (1975) 232–260.
[27] N. Sweed, R. Wilhelm, Parametric pumping: separations via thermal direct mode, Ind. Eng. Chem. Fund. 8 (1969) 221–231.
[28] P. Varhol, User-Centerd Application Design with Visual Basic, Wiley, New York, 1995, pp. 215–242.
[29] P. Wankat, Continuous recuperative mode parametric pumping, Ind. Eng. Chem. Fund. 12 (1978) 372–380.
[30] R. Wilhelm, A. Rice, A. Bendelius, 'Parametric pumping' a dynamic principle for separating fluid mixtures, Ind. Eng. Chem. Fund. 7 (1968a) 337–349.
[31] R. Wilhelm, N. Sweed, Parametric pumping: separation of mixture of toluene, Parametric pumping: separation of mixture of toluene and n-heptane, Science 159 (1968) 522–524.